Journal of Alloys and Compounds 502 (2010) 365–370

Contents lists available at ScienceDirect

Journal of Alloys and Compounds

journal homepage: www.elsevier.com/locate/jallcom

Controlling the size and size distribution of magnetite nanoparticles on carbon nanotubes

D. Shi, J.P. Cheng*, F. Liu, X.B. Zhang

Department of Materials Science and Engineering, State Key Laboratory of Silicon Materials, Zhejiang University, Hangzhou 310027, China

ARTICLE INFO

Article history:
Received 11 February 2010
Received in revised form 13 April 2010
Accepted 24 April 2010
Available online 4 May 2010

Keywords:
Nanostructured materials
Chemical synthesis
Sintering
Magnetization
Transmission electron microscopy

ABSTRACT

Nanocomposites composed of carbon nanotubes (CNTs) and magnetite (Fe_3O_4) nanoparticles were fabricated by using ethylene glycol as reductant at 160 °C. The composites were subsequently annealed under different temperatures in an inert atmosphere. The products were characterized by transmission electron microscopy (TEM), high resolution TEM, X-ray diffraction (XRD) and Fourier transform infrared (FTIR) spectroscopy. The results showed that the Fe_3O_4 transformed from amorphous phase into single crystalline nanoparticles after annealing and that the annealing temperature played a crucial role in controlling the size and the size distribution of Fe_3O_4 nanoparticles. The average size of Fe_3O_4 nanoparticles increased with increasing annealing temperature. Meanwhile, the size distribution of nanoparticles became wide with the increase of temperature. It was caused by the gradual decomposition of oleate groups attached on the CNT surface. Magnetic hysteresis loop measurements revealed that crystalline Fe_3O_4/CNTs displayed superparamagnetic behavior under room temperature.

1. Introduction

Magnetite (Fe_3O_4) nanoparticles have been applied in a variety of fields, such as ferrofluid technology [1,2], biomedicine [3], information storage [4], and environmental engineering [5]. Small sizes, uniform morphologies, soft magnetisms and high dispersity are typically required for the applications of magnetic nanoparticles because of the dependence of magnetic properties on the morphologies of nanoparticles. When the size of Fe_3O_4 nanoparticles is very small, the size of single magnetic domain is equal to that of each particle. Fe_3O_4 nanoparticles usually exhibit superparamagnetic property [6,7]. Therefore, the fabrication of Fe_3O_4 nanoparticles attracts a lot of interest.

In recent years, carbon nanotubes (CNTs) have also captured much attention worldwide due to their unique properties and potential applications in many practical fields [8,9]. Many efforts have been devoted to the synthesis of nanocomposites using CNTs due to their synergistic and hybrid properties as components, which have various applications such as reinforcement fibers, novel catalysts and potential electronic nanodevices [10–14]. Dispersing particles on the sidewalls of CNTs can make solid nanoparticles achieving a high dispersion degree. Thus, a variety of CNTs-based nanocomposites have been fabricated, which may be promising for applications in electronic devices [15].

Various chemistry-based methods have been developed to prepare Fe_3O_4/CNTs magnetic nanomaterials [13,16]. Though co-precipitation method is popular and simple, it has several disadvantages such as relatively poor crystallinity and magnetic properties, susceptibility to the air oxidation and the fixed stoichiometry ratio of Fe(II) to Fe(III) [17]. Polyol process is another versatile chemical approach, which employs polyols as solvent and reducing agent, as well as stabilizer to reduce metal salts to nanoparticles. For example, Cai and Wan [18] have successfully synthesized Fe_3O_4 nanoparticles in liquid polyols. Zhang et al. [19] also reported the preparation of monodisperse Fe_3O_4 sub-microspheres using ethylene glycol (EG) as both reducing agent and solvent. The advantages of polyols approach are the easily controlled experimental conditions, simplicity and less material consuming. While considerable successes have been achieved in the preparation of Fe_3O_4/CNTs nanocomposites, producing Fe_3O_4 nanoparticles with uniform size and controlling their size distribution, however, have consistently been big challenges. Hence, an easy and reliable process would be desirable to control the dispersion and size of Fe_3O_4 nanoparticles, especially in the case that the average particle size is smaller than 10 nm [17].

This paper reports a simple polyols method for the synthesis of Fe_3O_4/CNTs nanocomposites. The effects of the annealing temperature on the size and size distribution of the particles have also been investigated.

* Corresponding author. Tel.: +86 571 87951411; fax: +86 571 87951411.
E-mail addresses: chengjp@zju.edu.cn, chengjp@zju.edu.cn (J.P. Cheng).

0925-8388/$ – see front matter © 2010 Elsevier B.V. All rights reserved.
doi:10.1016/j.jallcom.2010.04.169

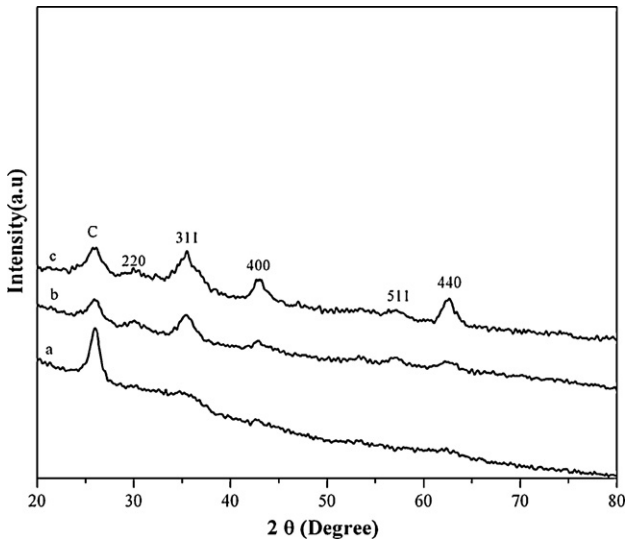

Fig. 1. XRD patterns of sample S1 (curve *a*), S2 (curve *b*), and S3 (curve *c*).

2. Experimental

2.1. Synthesis

Multi-walled CNTs were prepared by chemical vapor deposition method, where Fe–Co bimetallic catalyst supported on nanocrystalline $CaCO_3$ and acetylene were used as catalyst and carbon precursor, respectively. After reaction at 750 °C for 20 min, CNTs were obtained [20]. For the purification and functionalization, pristine CNTs were boiled in concentrated nitric acid for 4 h to get oxygenated groups on the external surface of CNTs, similar to previous reports [21,22]. Subsequently, the CNTs product was washed with adequate deionized water to remove residual acid and filtered, and then dried at 100 °C for 12 h.

In a typical procedure for the synthesis of Fe_3O_4/CNTs nanocomposite, 0.2 g CNTs and 3.333 g sodium oleate were added into a round-bottomed flask filled with 222 ml distilled water. The flask was sonicated for 30 min to get a CNT suspension. Separately, 1.4738 g of $Fe(NO_3)_3{\cdot}9H_2O$ was dissolved in 166 ml ethanol. The Fe-containing ethanol solution was added into the CNT suspension. Then, the mixture was slowly heated to 75 °C under vigorous stirring for 1 h. After cooling down to room temperature, black precipitate was obtained after filtration. The black precipitate was dried at 100 °C for 12 h. The dry product and 3.6 g sodium oleate were dispersed in 100 ml EG under vigorous stirring. The EG suspension was transformed into a sealed reactor under N_2 flow and heated to 160 °C with constant agitation for 2 h. After rinsing by ethanol, the Fe_3O_4/CNTs nanocomposite was obtained, which was named as sample S1.

Subsequently, annealing treatment was conducted under different temperatures. For comparison, sample S1 was heated in an argon flow at 300 °C and 600 °C for 30 min to obtain products named as sample S2 and sample S3, respectively.

2.2. Characterization

Transmission electron microscope (TEM, Philips CM200) was used to observe the Fe_3O_4/CNTs nanocomposites. The phase structures of the products were recorded by powder X-ray diffraction (XRD, X'Pert PRO) with Cu*K*α radiation. Field emission scanning electron microscope (FESEM, Hitachi S-4800) equipped with an energy dispersive X-ray spectrometer (EDS) was employed for examination on the morphology and elemental analysis of the products. FTIR spectra of the products were obtained using a BRUKER VECTOR 22 FTIR spectrometer (Germany) by dispersing nanocomposite in KBr and pressed as pellets. The magnetic properties of the products were obtained from hysteresis loops recorded in a vibrating sample magnetometer (VSM) at room temperature.

3. Results and discussion

Fig. 1 displays XRD patterns of Fe_3O_4/CNTs nanocomposites, in which the diffraction peak at 26.4° is due to the (0 0 2) diffraction of CNTs. According to PDF Cards 65-3107, the reflection peaks at the 2θ values of 30.0°, 35.4°, 43.1°, 57.0° and 62.6° can be assigned to (2 2 0), (3 1 1), (4 0 0), (5 1 1) and (4 4 0) crystal planes of cubic magnetite, respectively. However, diffraction analysis alone cannot distinguish between the cubic magnetite and maghemite because

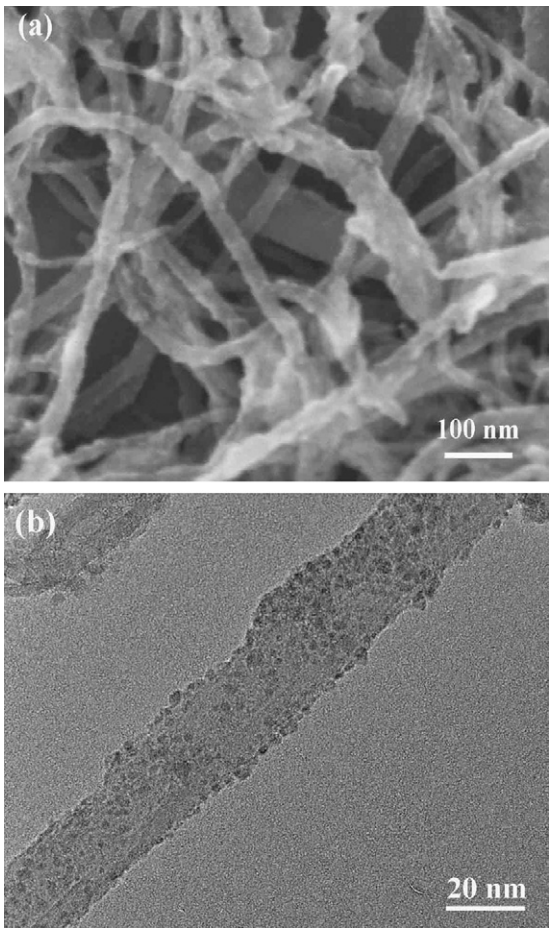

Fig. 2. SEM and TEM images of sample S1.

of their similarity in structure and lattice parameters. To further prove the composition of the composites, FTIR spectra were examined and shown in Fig. 6. The broadening of the peaks is primarily attributed to poor crystallinity as well as small crystal size. In curve *a*, the intensities of the peak of magnetite phase in sample S1 were thoroughly depressed, implying that the magnetite was amorphous due to the low growth temperature. While samples S2 and S3 exhibited in curves *b* and *c* clearly present the typical peaks of magnetite, respectively. Thus, we conclude that the crystallinity of the magnetite phase could be improved by thermal annealing [23]. However, the full width at half maximum of the magnetite peaks is still wide, suggesting that the crystal sizes of the magnetite are quite small.

The morphology and size distribution of Fe_3O_4 nanoparticles were examined by SEM and TEM observation. Fig. 2 shows typical SEM and TEM micrographs of sample S1. It is noticeable that a large number of nanoparticles are deposited and distributed homogeneously on the external surface of CNTs. Fig. 2b presents a typical TEM image of an individual CNT with a high magnification, in which extremely small particles, about 3 nm in diameters and exhibiting irregular shapes, are adhered on the nanotube. Though we had tried high resolution TEM (HRTEM) observation to investigate these particles, it was impossible to obtain an image with clear lattice fringes. Thus, these nanoparticles are amorphous, consistent with the XRD analysis. The elemental analysis by EDS proved that sample S1 contained C, Fe and O. The content of Fe in the composite was about 14% in weight.

The as-synthesized nanoparticles in sample S1 could be easily transformed into crystalline Fe_3O_4 through high temperature

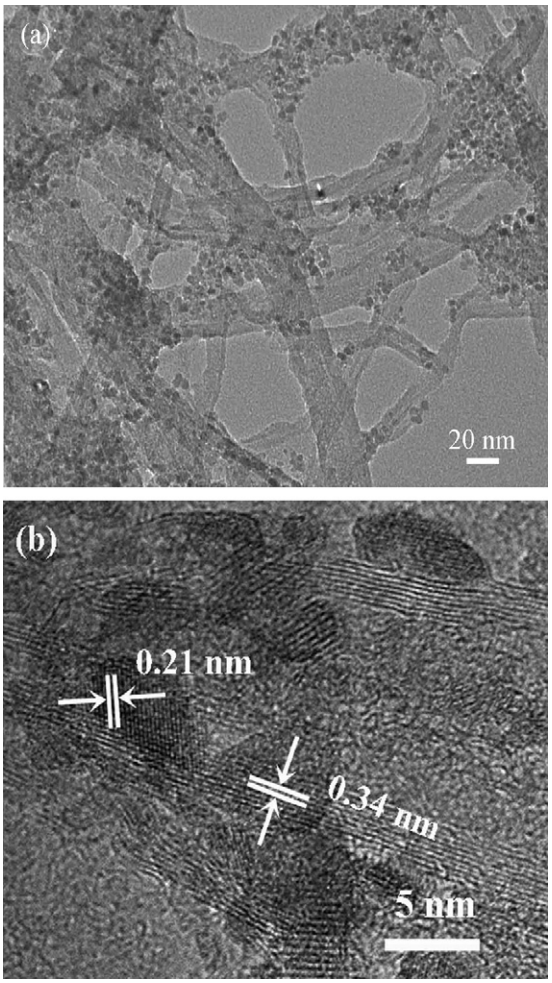

Fig. 3. TEM and HRTEM images of sample S2.

treatment in an inert atmosphere. Fig. 3 shows TEM and HRTEM images of sample S2. Fig. 3a reveals that spherical Fe_3O_4 nanoparticles with diameters of *ca.* 5 nm are densely distributed on the surface of CNTs. The interaction between Fe_3O_4 particles and CNTs was strong, as few individual particles were observed on the copper grids suffering from repeated washing and sonicating in the process. The crystalline nature of Fe_3O_4 nanoparticles is further revealed in a representative HRTEM image in Fig. 3b. The single crystalline Fe_3O_4 particles are confirmed. The parallel lattice fringes space measured from the image is about 0.21 nm, corresponding to the lattice constant of (4 0 0) planes of magnetite.

Fig. 4a shows a typical TEM image of sample S3, which indicates that CNTs are decorated with Fe_3O_4 nanoparticles. The diameter of the particles with spherical shapes is estimated to be *ca.* 10 nm. More detailed structural information of the particles was examined by HRTEM analysis, as shown in Fig. 4b. Clear lattice fringes of CNTs and Fe_3O_4 are observed, indicating that the single crystalline Fe_3O_4 particles are formed. The measured spacing of the crystallographic planes is about 0.48 nm, which is close to that of the (1 1 1) planes of magnetite crystals.

The size histograms of Fe_3O_4 particles on the surface of CNTs are shown in Fig. 5. Fig. 5a–c presents the size distribution of the nanoparticles in samples S1, S2 and S3, respectively. More than 100 nanoparticles were counted to determine the size distribution and average size of the nanoparticles from TEM measurements. The values of average size of Fe_3O_4 particles are the number averaged diameters in samples. The averaged particle size for samples S1, S2 and S3 are 3.1, 5.8 and 9.4 nm, respectively. The size distribution of Fe_3O_4 nanoparticles for sample S1 is in a narrow range from 2 to 5 nm, whereas those for samples S2 and S3 are in wide ranges from 3.5 to 7.5 nm, 6 to 16 nm, respectively. The size distribution of Fe_3O_4 particles before annealing is narrow (sample S1), whereas, after heat treatment their size distribution becomes relatively wide. It is obvious that the mean size and size distribution of Fe_3O_4 particles have a direct relationship with annealing temperature. The higher temperature of treatment is, the larger average size and wider distribution of particles are. Therefore, the size and size distribution of magnetite nanoparticles on the surface of CNTs can be easily controlled by varying the annealing temperatures.

FTIR spectra of samples S1, S2 and S3 were examined and presented in Fig. 6. As shown in Fig. 6(a) for sample S1, two characteristic bands at 2921, 2851 cm^{-1} of C–H vibrations and the bands at 1532, 1429 cm^{-1} of COO^- stretching can corroborate the attachment of oleate on the CNTs. The wavenumbers of COO^- at 1532, 1429 cm^{-1} are somewhat lower than those of sodium oleate (1562, 1450 cm^{-1} [6]), respectively, which can be explained by the high positive charge of ferric ion. As shown in Fig. 6(b) for sample S2, these characteristic absorption peaks of oleate are still observed with their intensities remarkably decreased, compared to those in Fig. 6(a). While for sample S3 in which the annealing temperature was fixed at 600 °C, the bands of C–H vibrations disappeared, indicating that oleate was decomposed completely, as shown in Fig. 6(c). The residual COO^- stretching band at 1586 cm^{-1} should be assigned to nitric acid pre-treatment. These changes of oleate group implied that the decomposition of oleate to a great extent related with annealing temperature. Oleate was completely decomposed under 600 °C from FTIR spectra, while an annealing temperature of 300 °C was not sufficient [24].

As seen from FTIR spectra in Fig. 6, the peaks at 583 and 709 cm^{-1} are the stretching vibration due to the interactions of Fe–O–Fe in Fe_3O_4 and γ-Fe_2O_3 (maghemite), respectively. The intensity of Fe–O–Fe absorption band of Fe_3O_4 is much stronger than that of γ-Fe_2O_3, suggesting that the main phase of the nanoparticles is Fe_3O_4. The existing of a small fraction of γ-Fe_2O_3 may be caused by the oxidation of magnetite nanoparticles by oxygen-containing groups attached on the oxidized CNTs [25], owing to their small size and high surface energy. It is known that maghemite is similar to magnetite in structure and lattice parameters. Thus, it was not easy to identify maghemite from magnetite simply based on conventional XRD patterns in Fig. 1.

As Section 2 described, the preparation of Fe_3O_4/CNTs nanocomposites is a multi-stepped process, in which various chemical reactions are involved. Nitric acid treatment would introduce carboxylic groups (–COOH) and hydroxyl groups (–OH) onto the surface of CNTs [20]. When CNTs were suspended into sodium oleate aqueous solution, the hydrophobic chain of oleate molecules could be effectively anchored onto CNTs through hydrophobic interaction with the sidewall of the CNTs and thereby the hydrophilic groups would extend into solution [26,27]. After the addition of the ethanol solution of $Fe(NO_3)_3$, ferric ions reacted with oleate to form ferric oleate which were then attached onto the surface of CNTs [6]. Besides, some ferric ions were attached on the CNTs through the functional groups, such as carboxylic groups (–COOH) [28]. Subsequently, the ferric ions were in situ reduced into Fe_3O_4 by EG with the assistance of sodium oleate [29]. The Fe_3O_4 was amorphous in phase due to the low reaction temperature in our case, though Liu et al. [13] reported that crystalline magnetite was formed by the reduction of EG at 200 °C in autoclave. During the process of heat treatment, the decomposition of oleate gradually occurred with increasing temperature. Those particles that lost the interlinked molecules, i.e. oleate, tended to aggregate to form bigger ones. Thus the average particle size of sample S2 is larger than that of sample S1. Meanwhile, the crystallization of Fe_3O_4 nanopar-

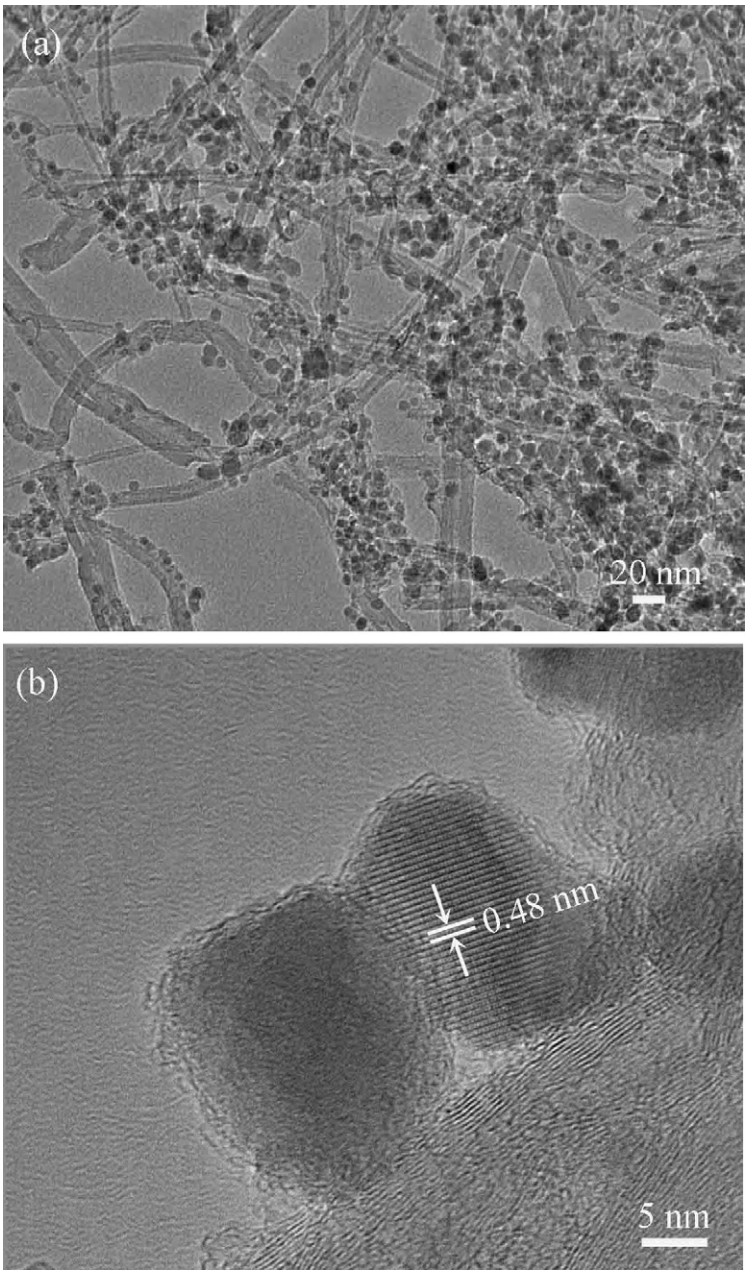

Fig. 4. TEM and HRTEM images of sample S3.

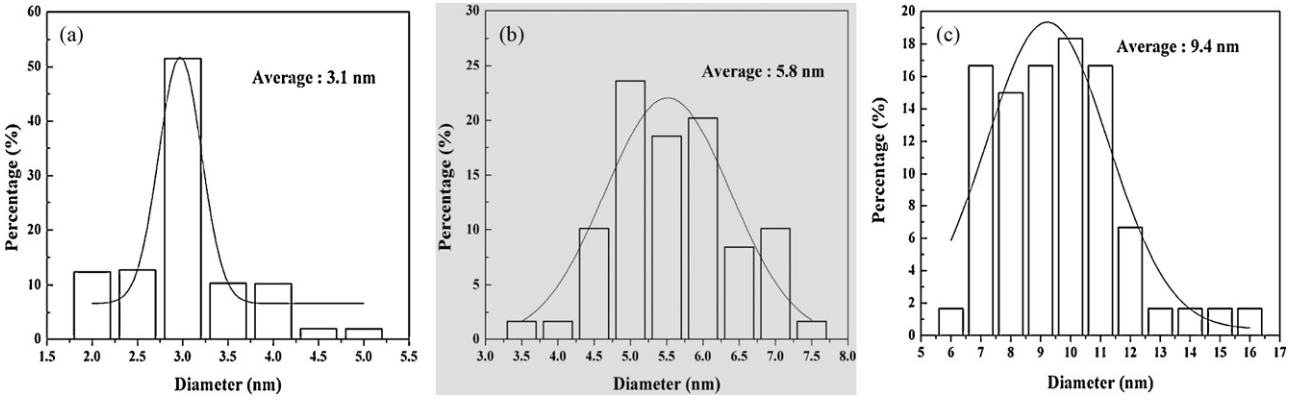

Fig. 5. Histograms indicating the size distribution for sample S1 (a), sample S2 (b), and sample S3 (c) measured from the corresponding TEM images

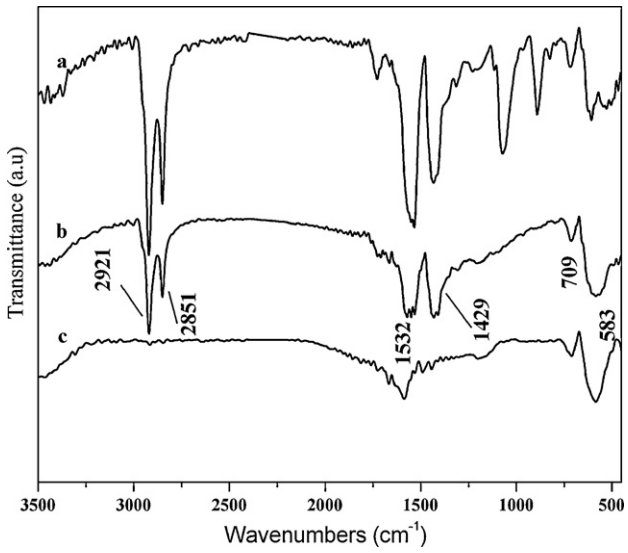

Fig. 6. FTIR spectra of samples S1 (curve *a*), S2 (curve *b*), and S3 (curve *c*).

ticles started, which has been verified by the XRD results in Fig. 1. In the case of sample S3, the particle size dramatically increased due to the loss of the stabilization ability caused by the elimination of oleic groups at 600 °C. Because the oleic groups completely decomposed at 600 °C, chemical bond between CNTs and Fe_3O_4 nanoparticles disappeared. The retained interaction between CNTs and Fe_3O_4 nanoparticles was van der waals force.

TEM images have clearly proved that the size and size distribution of Fe_3O_4 nanoparticles depended on the annealing temperature. These particles in samples S2 and S3 tended to aggregate during the annealing process, and the size distribution of these particles also increased with the increase of annealing temperature. All these phenomena could be explained by the changes of oleate on CNTs surface, indicating a simple and promising route to achieve magnetic nanocomposite with reasonable size control.

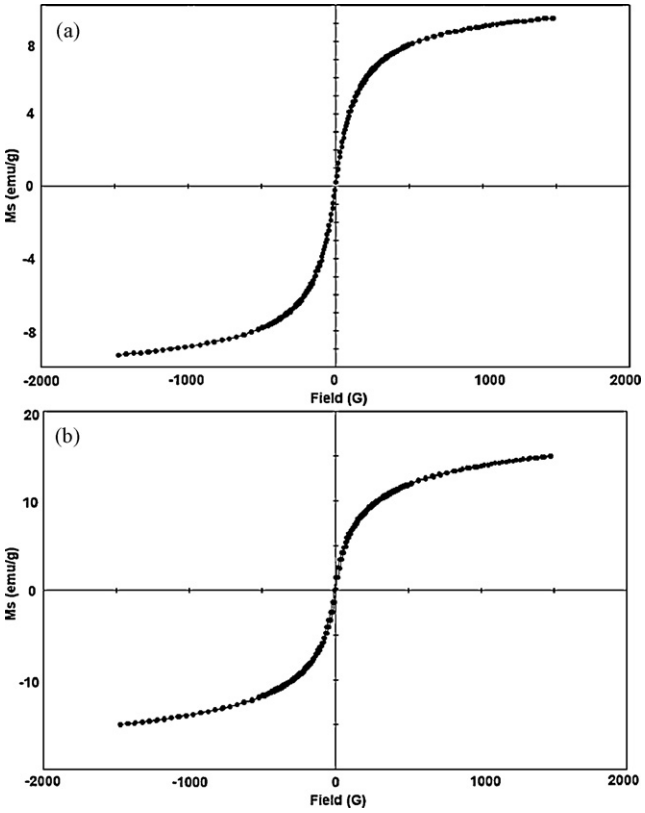

Fig. 7. Magnetic hysteresis loops of sample S2 (curve *a*) and S3 (curve *b*).

The magnetic property of Fe_3O_4/CNTs nanocomposites was investigated by VSM. Fig. 7 illustrates magnetization curves for sample S2 (Fig. 7a) and S3 (Fig. 7b), which were taken at 25 °C. The saturation magnetizations of samples S2 and S3 are 9.3 and 17 emu g^{-1}, respectively, significantly smaller than that of bulk Fe_3O_4 (93 emu g^{-1}) [22]. The low magnetization is likely attributed to the presence of non-magnetic components in the composites. The increase in the saturation magnetization is attributed to the increase in the crystallinity of Fe_3O_4 nanoparticles. The curve for sample S2 in Fig. 7a has no coercivity, suggesting the superparamagnetic nature of the nanocomposite. However, very low coercivity appeared in the curve for sample S3 in Fig. 7b and the value is determined to be 54 Oe. This may be explained by the increase of both particle size and crystallinity, because the magnetic behavior of Fe_3O_4 is very sensitive to the particle size.

4. Conclusions

In summary, nanocomposites composed of CNTs and Fe_3O_4 nanoparticles were fabricated using EG as reductant under 160 °C. The as-prepared Fe_3O_4 nanoparticles were amorphous with a small size and narrow size distribution. Through annealing treatment under different temperatures, it would cause a phase transition from amorphous Fe_3O_4 to crystalline nanoparticles. The average particle size of Fe_3O_4 was increased with increasing temperature and their size distribution was wider under a higher temperature. These changes were dependent on the decomposition of oleic groups attached on the CNTs surface. Magnetic measurements showed that Fe_3O_4/CNTs nanocomposites had superparamagnetic characteristics.

Acknowledgements

This work was financially supported by National Natural Science Foundation of China (No. 50571087) and Natural Science Foundation of Zhejiang Province (No. Y4080129).

References

[1] H.T. Pu, F.J. Jiang, Towards high sedimentation stability: magnetorheological fluids based on CNT/Fe_3O_4 nanocomposites, Nanotechnology 16 (2005) 1486–1489.
[2] K. Raj, R. Moskowitz, Commercial applications of ferrofluids, J. Magn. Magn. Mater. 85 (1990) 233–245.
[3] B. Feng, R.Y. Hong, Y.J. Wu, G.H. Liu, L.H. Zhong, Y. Zheng, J.M. Ding, D.G. Wei, Synthesis of monodisperse magnetite nanoparticles via chitosan-poly(acrylic acid) template and their application in MRI, J. Alloys Compd. 473 (2009) 356–362.
[4] Z. Liu, J. Wang, D.H. Xie, G. Chen, Polyaniline coated Fe_3O_4 nanoparticle carbon nanotube composite and its application in electrochemical biosensing, Small 4 (2008) 462–466.
[5] K.Y. Dong, S.L. Su, Y.Y. Jackie, Synthesis and applications of magnetic nanocomposite catalysts, Chem. Mater. 18 (2006) 2459–2461.
[6] X.T. Wen, J.X. Yang, B. He, Z.W. Gu, Preparation of monodisperse magnetite nanoparticles under mild conditions, Curr. Appl. Phys. 8 (2008) 535–541.
[7] G.Y. Li, Y.R. Jiang, K.L. Huang, P. Ding, J. Chen, Preparation and properties of magnetic Fe_3O_4-chitosan nanoparticles, J. Alloys Compd. 466 (2008) 451–456.
[8] J.P. Cheng, X.B. Zhang, F. Liu, J.P. Tu, Y. Ye, Y.J. Ji, C.P. Chen, Synthesis of Carbon Nanotubes Filled with Fe_3C Nanowires by CVD with Titanate Modified Palygorskite as Catalyst, Carbon 41 (2003) 1965–1970.
[9] J.P. Cheng, X.B. Zhang, J.P. Tu, X.Y. Tao, Y. Ye, F. Liu, Catalytic chemical vapor deposition synthesis of helical carbon nanotubes and triple helices carbon nanostructure, Mater. Chem. Phys. 95 (2006) 12–15.
[10] K.R. Reddy, B.C. Sin, C.H. Yoo, W. Park, K.S. Ryu, J.S. Lee, D. Sohn, Y. Lee, A new one-step synthesis method for coating multi-walled carbon nanotubes with cuprous oxide nanoparticles, Scripta Mater. 58 (2008) 1010–1013.

[11] M.H. Chen, Z.C. Huang, G.T. Wu, G.M. Zhu, J.K. You, Z.G. Lin, Synthesis and characterization of SnO carbon nanotube composite as anode material for lithium ion batteries, Mater. Res. Bull. 38 (2003) 831–836.
[12] J.P. Cheng, X.B. Zhang, Y. Ye, J.P. Tu, F. Liu, X.Y. Tao, H.J. Geise, G. Van Tendeloo, Production of carbon nanotubes with marine manganese nodule as a versatile catalyst, Micropor. Mesopor. Mater. 81 (2005) 73–78.
[13] Y. Liu, W. Jiang, S. Li, Z.P. Cheng, D. Song, X.J. Zhang, F.S. Li, Attachment of magnetic nanoparticles on carbon nanotubes using oleate as an interlinker molecule, Mater. Chem. Phys. 116 (2009) 438–441.
[14] P. Chen, X. Wu, J. Lin, K.L. Tan, Synthesis of Cu nanoparticles and microsized fibers by using carbon nanotubes as a template, J. Phys. Chem. B 103 (1999) 4559–4561.
[15] J.Y. Lee, K. Liang, K.H. An, Y.H. Lee, Nickel oxide/carbon nanotubes nanocomposite for electrochemical capacitance, Syn. Met. 150 (2005) 153–157.
[16] S.W. Ko, M.K. Hong, H.J. Choi, B.H. Ryu, Synthesis of carbon nanotubes and iron oxide nanoparticles in MW plasmatorch with $Fe(CO)_5$ in gas feed, IEEE T. Magn. 45 (2009) 2503–2506.
[17] S. Zhao, S. Asuha, One-pot synthesis of magnetite nanopowder and their magnetic properties, Powder Technol. 197 (2010) 295–297.
[18] C. Wei, J.Q. Wan, Facile synthesis of superparamagnetic magnetite nanoparticles in liquid polyols, J. Colloid Interf. Sci. 305 (2007) 366–370.
[19] J.H. Zhang, Q.H. Kong, W.L. Lu, H. Liu, Synthesis, characterization and magnetic properties of near monodisperse Fe_3O_4 sub-microspheres, Chinese Sci. Bull. 54 (2009) 2434–2439.
[20] J.P. Cheng, X.B. Zhang, Z.Q. Luo, F. Liu, Y. Ye, W.Z. Yin, W. Liu, Y.X. Han, Carbon nanotube synthesis and parametric study using $CaCO_3$ nanocrystals as catalyst support by CVD, Mater. Chem. Phys. 95 (2006) 5–11.
[21] J.P. Cheng, X.B. Zhang, Y. Ye, Synthesis of nickel nanoparticles and carbon encapsulated nickel nanoparticles supported on carbon nanotubes, J. Solid State Chem. 179 (2006) 91–95.
[22] J.P. Cheng, X.B. Zhang, G.F. Yi, Y. Ye, M.S. Xia, Preparation and magnetic properties of iron oxide and carbide nanoparticles in carbon nanotube matrix, J. Alloys Compd. 455 (2008) 5–9.
[23] B. Gao, C. Peng, G.Z. Chen, G.L. Puma, Photoelectro catalysis enhancement on carbon nanotubes/titanium dioxide ($CNTs/TiO_2$) composite prepared by a novel surfactant wrapping sol–gel method, Appl. Catal. B: Environ. 85 (2008) 17–23.
[24] C.Y. Wang, J.M. Hong, G. Chen, Y. Zhang, N. Gu, Facile method to synthesize oleic acid-capped magnetite nanoparticles, Chinese Chem. Lett. 21 (2010) 179–182.
[25] Y.S. Kang, S. Risbud, J.F. Rabolt, P. Stroeve, Synthesis and characterization of nanometer-size Fe_3O_4 and γ-Fe_2O_3 particles, Chem. Mater. 8 (1996) 2209–2211.
[26] C. Richard, F. Balavoine, P. Schultz, T.W. Ebbesen, C. Mioskowski, Supramolecular self-assembly of lipid derivatives on carbon nanotubes, Science 300 (2003) 775–778.
[27] M.N. Zhang, L. Su, L.Q. Mao, Surfactant functionalization of carbon nanotubes (CNTs) for layer- by-layer assembling of CNT multi-layer films and fabrication of gold nanoparticle/CNT nanohybrid, Carbon 44 (2006) 276–283.
[28] L. Zhang, Q.Q. Ni, T. Natsuki, Y.Q. Fu, Carbon nanotubes/magnetite hybrids prepared by a facile synthesis process and their magnetic properties, Appl. Surf. Sci. 255 (2009) 8676–8681.
[29] H. Deng, X.L. Li, Q. Peng, X. Wang, J.P. Chen, Y.D. Li, Monodisperse magnetic single-crystal ferrite microspheres, Angew. Chem. Int. Ed. 44 (2005) 2782–2785.